11th Australasian Fluid Mechanics Conference
University of Tasmania, Hobart, Australia
14-18 December 1992

STUDY OF LAMINAR SEPARATION BUBBLES AT LOW REYNOLDS NUMBER UNDER VARIOUS CONDITIONS

Alex C.N. TAN and Douglass J. AULD

Department of Aeronautical Engineering
University of Sydney, NSW 2006, AUSTRALIA

ABSTRACT

An experimental investigation was conducted to study the structure of laminar separation bubbles formed on several aerofoils under various conditions. Measurements include surface pressure distribution, pressure fluctuation in the chordwise direction and surface normal boundary layer velocity obtained using a single hot-wire probe. Boundary layer results include mean velocity profiles, turbulence intensity profiles and energy spectra of the fluctuating velocity. Flow visualisation with smoke and liquid film was also used to investigate the flow structure in the separation region. Comparisons of the laminar bubble length of current and previous experimental data with semi-empirical theories have also been made.

INTRODUCTION

Low Reynolds number aerodynamics has recently drawn much attention in applications such as remotely Piloted Vehicles (RPVs), ultralight aircraft, sailplanes, wind turbines and turbomachinery blades.

At high Reynolds number, the boundary layer on an aerofoil rapidly becomes turbulent and in most cases is able to negotiate an adverse pressure gradient with minimum disturbance. Design and evaluation techniques for aerofoil sections at high Reynolds number are reasonably well developed. However for low Reynolds number, serious problems relating to boundary layer separation, transition and turbulent reattachment have been encountered.

Observations in the low Reynolds number range have shown that before boundary layer flows become turbulent, a circulatory motion of fluid commonly referred to as a "laminar separation bubble" forms as a result of laminar separation. This separation bubble affects the pressure distribution and the development of the turbulent boundary layer downstream and consequently, the performance of aerofoils at low Reynolds number depends strongly on it. As the turbulent boundary layer downstream of the bubble is usually thicker than that formed as a result of natural transition at high Reynolds number, the resulting drag is greater.

It has been observed that laminar separation bubbles are sensitive to parameters such as freestream turbulence (LeBlanc et al(1986), Robert (1980)), and acoustic disturbance (Collin(1981), Ahuja and Burrin(1984), Hsiao et al(1990)). Other factors that could also affect the characteristics of separation bubbles include pressure gradient, aerofoil geometry, surface roughness, and operational Reynolds number.

For turbomachinery which involves high levels of freestream turbulence, there is currently little experimental data involving separation bubbles. Experimental data relating the effect of surface roughness on separation bubbles is also scarce. The lack of experimental data investigating effects such as freestream turbulence level, the surface roughness and the magnitude of the adverse pressure gradient, motivated this research in which several aerofoils have been tested under some of these conditions. Measurements include mean and fluctuating surface pressure distribution in the chordwise direction, and surface normal boundary layer measurements using a single hot-wire probe. Boundary layer results include mean velocity profiles, turbulence intensity profiles and energy spectra of the fluctuating velocity. Flow visualisation with smoke and liquid film was also conducted to investigate the flow structure during separation and to confirm the hot-wire boundary layer measurements.

EXPERIMENTAL APPARATUS

All tests were carried out in the Department of Aeronautical Engineering 3ft x 4ft low speed, closed circuit wind tunnel. A manually controlled 3 degrees-of-freedom traversing mechanism was used to move a hot-wire probe towards the surface of a test aerofoil. The traversing mechanism had a resolution of 0.2mm in the freestream direction, 0.025mm in the vertical direction and 0.4 degree in rotation. Hot-wire measurements were obtained with a constant temperature anemometer. A single-sensor DISA 55P15 hot-wire probe was used. The anemometer output voltage signals were input to a personal computer via an Analog to Digital converter (12 bits). Hot-wire signals were sampled at rates between 5,000 Hz and 20,000 Hz depending on the operational Reynolds number. A two-dimensional Wortmann FX67-150K (modified) aerofoil was used in this study. The aerofoil had a 386mm chord to produce a relatively thick boundary layer. The span was equal to the wind tunnel width of 1.22m. The aerofoil had 135 pressure tappings distributed over the top and bottom surface. The model was mounted to the side wall of the wind tunnel and was rotatable to any required angle of attack.

The clean wind tunnel had a turbulence level of approximately 0.12%. Freestream turbulence was increased by introducing three different types of wire grids 1500mm in front of the aerofoil producing turbulence levels of approximately 0.42%, 0.90% and 1.20%. The aerofoil surface static pressure was measured using 2 sets of computer controlled scanivalves linked to 2 pressure transducers. Signals from the pressure transducers were recorded in a similar manner to the hot-wire signal.

EXPERIMENTAL RESULTS

Surface Static Pressure

Figure 1 shows the measured surface pressure coefficients of the upper surface at α=0° with a mid-chord short laminar separation bubble.

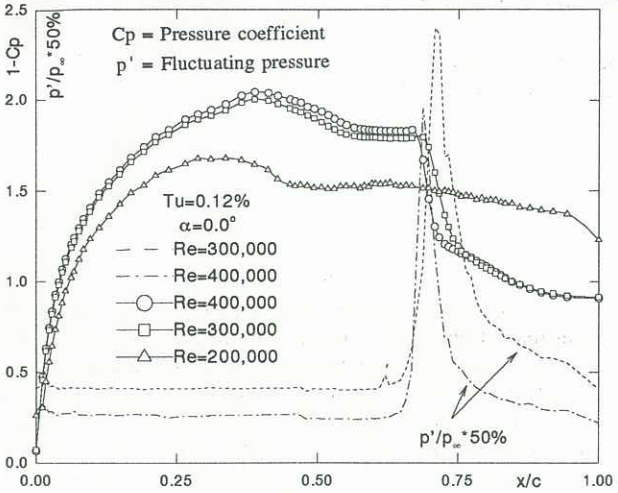

FIGURE 1. Pressure distribution and pressure fluctuation.

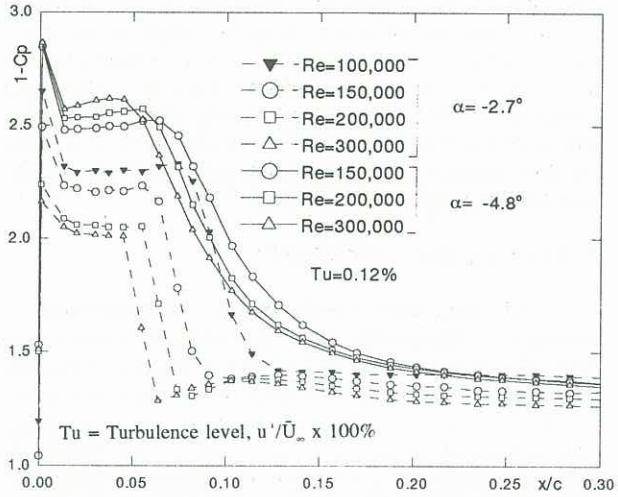

FIGURE 2. Pressure distribution

Figure 2 shows a leading edge short bubble at α=-2.7° and a leading edge long bubble at α=-4.8° of the lower surface. The existence of the separation bubble produces an approximate constant pressure plateau starting from the separation point until the transition region, followed by a sharp pressure rise in the turbulent bubble region blending into the turbulent boundary layer. The surface static pressure fluctuations (see Figure 3) start to increase as the flow moves towards the transition region and the fluctuation reaches a maximum just before the reattachment region. For the case of Re=200,000 at α=0°, the separation bubble fails to reattach to the surface resulting in a collapse of the pressure distribution and hence a large wake is formed. As Reynolds number increases, the separation bubble reattaches itself on the aerofoil surface. In all cases, increasing Reynolds number decreases the size of the laminar separation bubble. Increasing the freestream turbulence level from 0.12% to 0.42% causes the separated flow to reattach to the aerofoil surface showing similar characteristics to the case of increasing Reynolds number. Further increases in freestream turbulence level decreases the size of the bubble.

Flow Visualisation

To understand the extent of the laminar separation bubble, the location of the separation, transition and reattachment must be accurately determined. Surface and smoke flow visualisations were conducted to determine these locations. Surface flow visualisation used a mixture of titanium dioxide, oleic acid and kerosene and the mixture was sprayed onto the aerofoil surface producing a thin layer of oil film.

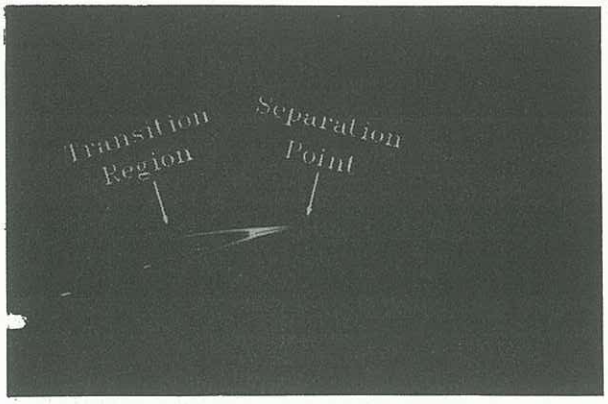

FIGURE 3. Smoke flow visualisation

Eucalyptus smoke vapour was bled aft of the separation point from small holes in the aerofoil surface. The smoke then moved upstream toward the separation point. The separation position was recorded using a cathetometer. Figure 3 shows the separation point obtained from the smoke flow visualisation technique. Although both techniques show the location of the separation point, smoke flow visualisation is the most accurate and reliable. The reattachment position can only be determined accurately through the surface flow visualisation technique.

Boundary Layer

Mean velocity and turbulence intensity profiles were calculated at various Reynolds number and various freestream turbulent levels. Equi-velocity contour plots ($\bar{u}/\bar{U}e$=0.3) shown in Figure 4,5 and 6 review an approximate outline shape of the two types of separation bubble. Short separation bubbles formed at mild pressure gradient. As pressure gradient increases, the short bubble (Figure 4,5) may burst and form a long separation bubble (Figure 6). In the case of a short bubble, the flow reattached itself to the aerofoil surface shortly after transition whereas the long bubble did not.

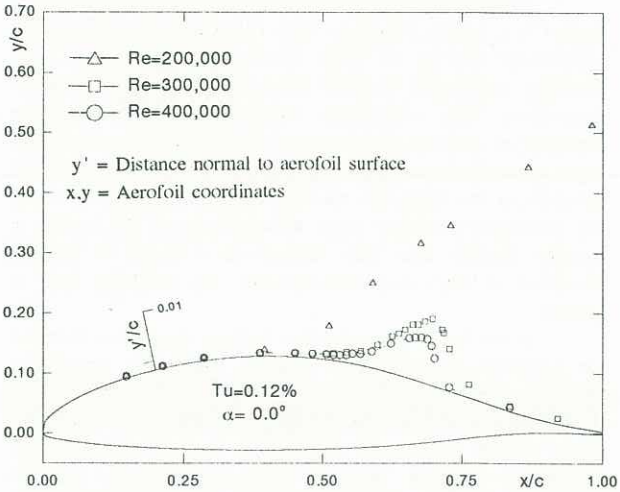

FIGURE 4. Equi-velocity contour (Short bubble)

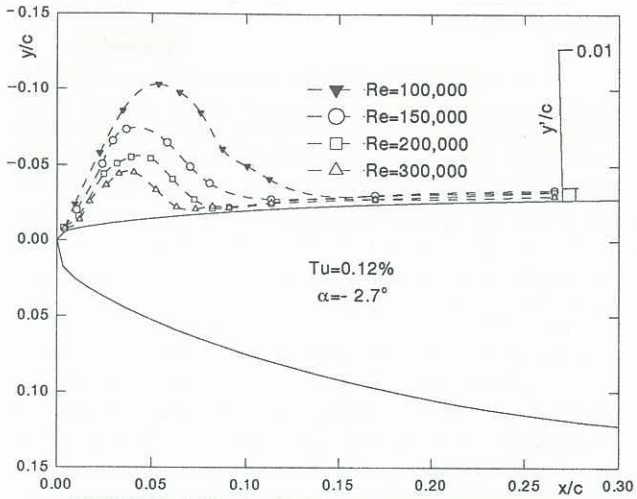

FIGURE 5. Equi-velocity contour (Short bubble)

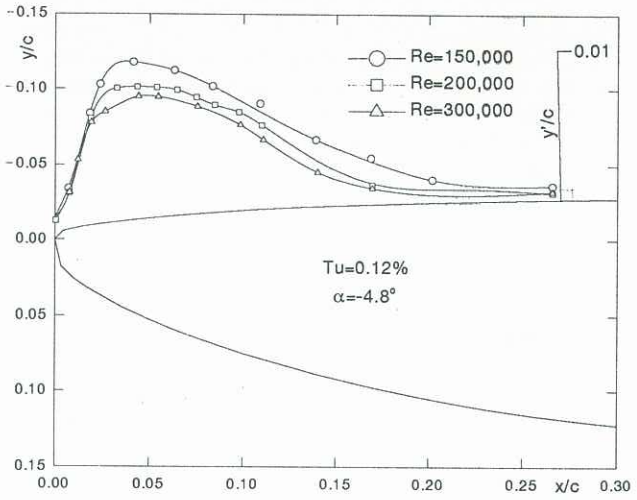

FIGURE 6. Equi-velocity contour (Long bubble)

Figure 7 shows the local maximum turbulence intensity profile of a short bubble and a long bubble at different chord locations. In the case of a short bubble, the maximum turbulence intensity occurs in the vicinity of the reattachment region where as the maximum value occurs much further forward in the bubble.

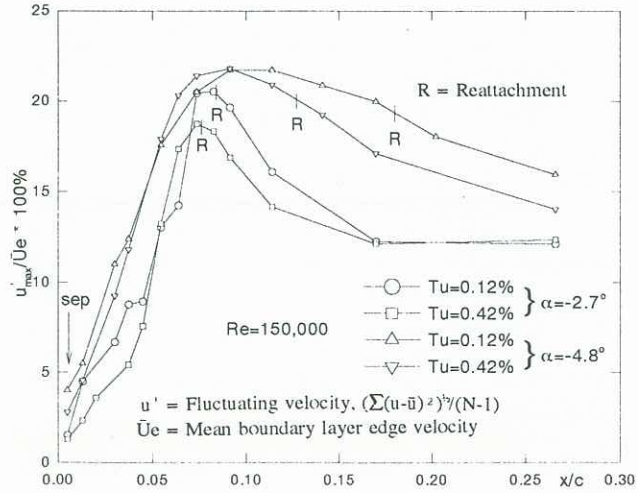

FIGURE 7. Turbulence intensity

Energy Spectra

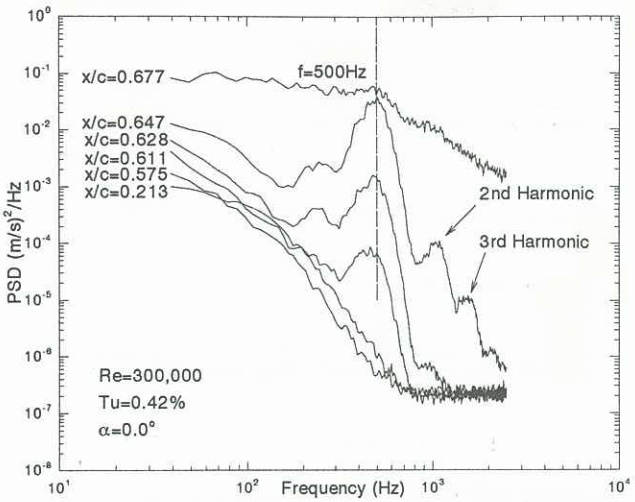

FIGURE 8. Power Spectral Density

To better understand the mode of transition within the separation bubble, the hot-wire signals were used to calculate the power spectral density using a Hanning window as shown in Figure 8. Power Spectra were calculated at the approximate location of maximum fluctuation level in the boundary layer, which corresponds to the position at which ū/Ūe=0.50. As the flow approaches transition, a distinct frequency peak (f≈500 Hz) starts to appear. Further aft to the reattachment region, the distinct frequency disappears and the signal shows high energy level turbulent mixing. The second, third and possibly the fourth harmonics of the distinct peak frequency are also evident in the transition region. Although increasing the turbulence level shortens the separation bubble, the distinct frequency near the transition remains undisturbed. With increasing Reynolds number, the distinct frequency value increases as well. The distinct frequency near transition is not well defined for the separation bubble formed at the leading edge compared to that formed near the mid-chord at high freestream turbulence level. Thus at high turbulence levels, the characteristic of the separation bubble also depends on the position where the bubble is formed.

The time signal from the hot-wire of a short bubble and a long bubble are shown in Figure 9 and Figure 10 respectively. Both signals are taken at the edge of the boundary layer at different locations of the separation bubble. The short bubble shows a laminar signal at the initial stage which then begins to oscillate at a distinct frequency with increasing amplitude further downstream and eventually breaks down into turbulence. For the case of a long bubble, an intermittent burst of oscillating wave starts at an early stage of the bubble. The intermittent bursting continues further downstream with increasing frequency until a more continuous oscillation with occasional bursts is found. Similar characteristics were observed by Gaster(1969) for a long

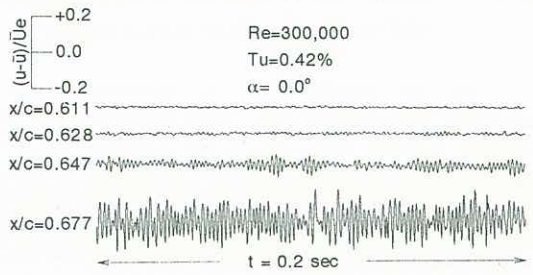

FIGURE 9. Time signal (short bubble)

bubble formed on a flat plate with the aid of an auxiliary aerofoil.

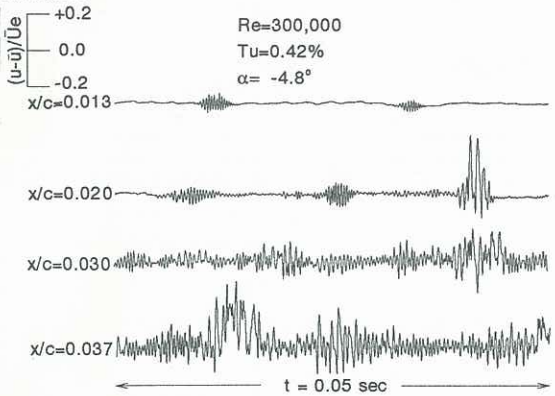

FIGURE 10. Time signal (long bubble)

Laminar Bubble Length

There have been previous attempts to derive semi-empirical theories to determine the size of the laminar portion of a laminar separation bubble. Horton(1969), Schmidt and Mueller's (1989) semi-empirical theories were used for comparison but do not conclusively agree with some of the current experimental data, especially at higher $Re\theta_{sep}$ as shown in Figure 11. The semi-empirical curve derived by the authors (Tan and Auld (1991)) earlier agreed reasonably well with current experimental data and experimental data obtained from various sources (Gaster (1969),Vincent de Paul (1972), O'Meara and Mueller (1987), Brendel and Mueller (1988), Tan and Auld (1991)-corrected data). The abovementioned semi-empirical theories should be applied with extreme caution since the experimental data obtained from the various sources shows quite a scatter, especially at higher $Re\theta_{sep}$. Different techniques for determining the separation and transition locations may be responsible for the scatter. Different wind tunnel conditions is another possible factor.

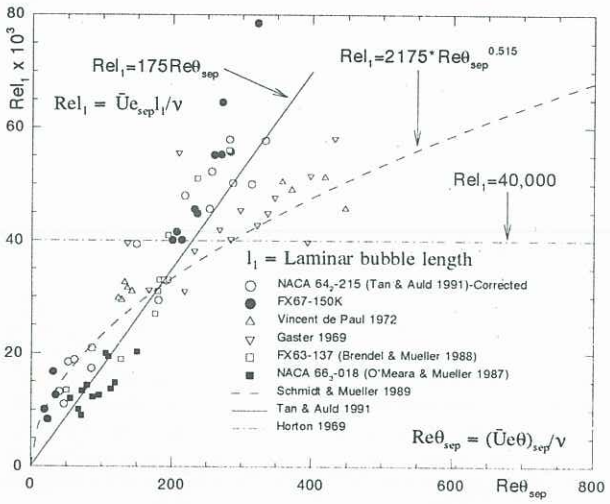

FIGURE 11. Laminar bubble length

For the current test, the separation point was determined using smoke flow visualisation results and the transition location was defined by examining the static pressure distribution, boundary layer edge velocity distribution, the equi-velocity contours and the power spectra of the hot-wire signal. The spacing of the pressure tapping locations and the chordwise step size hot-wire traverses were contributing factors to the uncertainty in the experimental results.

CONCLUSION

All experiments show that increased Reynolds number and increased freestream turbulence levels promote earlier transition within the separation bubble and hence shorten the size of the bubble. Increased turbulence levels increase the energy level in the boundary layer flow and hence in the case of α=0° at Re=200,000 the separation bubble reattaches itself to the aerofoil surface. A similar phenomenon was observed at Re=150,000. Although increased freestream turbulence levels and increased Reynolds number produce similar effects on the bubble length, the boundary distinct frequency in vicinity of the transition varies only with Reynolds number.

Current and previous experimental results do not conclusively match existing semi-empirical theories for determining the laminar bubble length. Other factors such as acoustic environment, aerofoil shape and curvature and the location where the separation bubble forms on the aerofoil possibly contribute to the differences.

Further investigations are being carried out in an effort to examine the growth rate within the laminar separation bubble through careful matching of Falkner-Skan solution of reverse flow and experimental data. A large range of parameters such as freestream turbulence level, surface roughness and pressure gradient with aerofoils of different shape and thickness are currently being investigated.

REFERENCES

Ahuja,K.K and Burrin,R.H (1984) Control of flow separation by sound, AIAA-84-2298.

Brendel,M and Mueller,T.J (1988) Boundary layer measurements on an airfoil at low Reynolds numbers, Journal of Aircraft, Vol 25, No.7, 612-617.

Collin,F.G(1981) Boundary layer control on wings using sound and leading edge serrations, AIAA Journal, Vol 19, No.2, 129-130.

Gaster,M (1969) The structure and behaviour of laminar separation bubbles, ARC R&M 3595.

Horton,G.P (1969) A semi-empirical theory for the growth and bursting of laminar separation bubbles. ARC CP No. 1073.

Hsiao,F.B et al(1990) Control of wall-separated flow by internal acoustic excitation, AIAA Journal, Vol 28, No.8, 1440-1446.

LeBlanc,P et al(1986) Boundary layer and performance characteristics from wind tunnel tests of a low Reynolds number Liebeck airfoil, Royal Aero. Soc. Conference on Low Reynolds Numbers 10^4<Re<10^6, 8.1-8.19.

O'Meara,M.M and Mueller,T.J(1987) Laminar separation bubble characteristics on a airfoil at low Reynolds numbers, AIAA Journal, Vol 25, No.8, 1033-1041.

Robert,W.B (1980) Calculation of laminar separation bubbles and their effect on airfoil performance, AIAA Journal, Vol 18, No.1, 25-31.

Schmidt,G and Mueller, T.J (1989) The analysis of low Reynolds number separation bubbles using semi-empirical methods, AIAA Journal, Vol 27, No.8, 993-1001.

Tan,A and Auld,D.J (1991) Experimental investigation of laminar to turbulent boundary layer transition with separation bubbles at low Reynolds number. Royal Aeronautical Society Conference on Boundary Layer Transition and Control, 14.1-14.5.

Vincent De Paul,M (1972) Prevision du decrochage d'un profil d'aile en ecoulement incompressible, AGARD CP-102.